analytical chemistry

ARTICLE

pubs.acs.org/ac

Chemical, Thermal, and Electric Field Induced Unfolding of Single Protein Molecules Studied Using Nanopores

Kevin J. Freedman,[†] Maike Jürgens,[∥] Anmiv Prabhu,[‡] Chi Won Ahn,[⊥] Per Jemth,[∥] Joshua B. Edel,[#] and Min Jun Kim[*,‡,§]

Departments of [†]Chemical and Biological Engineering, [‡]Biomedical Engineering, and [§]Mechanical Engineering, Drexel University, Philadelphia, Pennsylvania 19104, United States

[∥]Department of Medical Biochemistry and Microbiology, Uppsala University, Uppsala, Sweden

[⊥]NEMS-BIO Team, National Nanofab Center, Deajeon, Korea

[#]Department of Chemistry, Imperial College London, South Kensington, London, United Kingdom

ABSTRACT: Single-molecule experimental techniques have recently shown to be of significant interest for use in numerous applications in both the research laboratory and industrial settings. Although many single-molecule techniques exist, the nanopore platform is perhaps one of the more popular techniques due to its ability to act as a molecular sensor of biological macromolecules. For example, nanopores offer a unique, new method for probing various properties of proteins and can contribute to elucidating key biophysical information in conjunction with existing techniques. In the present study, various forms of bovine serum albumin (BSA) are detected including thermally refolded BSA, urea-denatured BSA, and multiple forms of BSA detected at elevated electric field strengths (with and without urea). We also provide excluded volume measurements for each of these states that normally are difficult to obtain due to unknown and unstable protein conformations.

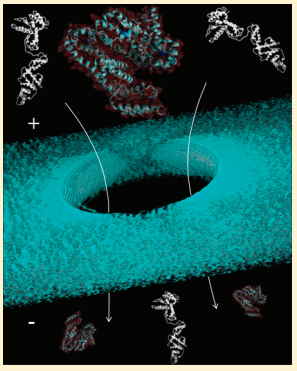

Single-molecule science is a relatively new and exciting field in which the physicochemical properties of an analyte are studied for individual molecules. The methods used to perform such analyses are very different from traditional techniques, which rely on ensemble averaging (obtaining a signal from more than one molecule). Although averaging over many molecules is an extremely useful and reliable experimental paradigm, some questions simply cannot be answered this way and therefore necessitate a slightly different approach. For example, if one wanted to detect a subset of very rare protein folding events within a larger population, single-molecule techniques would be absolutely essential. Another specific example relates to the ubiquitous biological phenomenon of a protein traveling through a pore, such as in the mitochondrial membrane or endoplasmic reticulum. The folding and unfolding of proteins as they pass through a pore are inherently single-molecule events, which are not completely understood.[1] Experimentally, the nanopore platform is an ideal tool for use in such experiments as the energetics of biomolecules going through individual pores can be studied.[2]

Aside from answering purely scientific questions, more practical benefits of using nanopores as a single-molecule sensor include the following: (a) low analyte volumes are needed, (b) they can work at both low and high concentrations of analyte depending on requirements, (c) statistics on subpopulations can be easily extracted, and (d) solid-state nanopores can be integrated into lab-on-a-chip instruments for high-throughput, inexpensive, electrical detection of biomolecules.[3] Detecting low concentrations of a protein or protein state is not only a large limiting factor in current sensing techniques but also has important applications in studying the behavior of proteins at their physiological concentration.[4] Since physiological concentrations can be quite low (subnanomolar[5]), methods to study protein behavior under these conditions are important and can help understand natural biological processes as well as pathological ones, such as protein misfolding and fibril formation in Alzheimer's disease.[6] Furthermore, since aggregation is a concentration-dependent process, the lifetime of the preaggregate state(s) is increased at lower concentrations.[7,8]

Historically, solid-state nanopores, often formed in a thin silicon nitride membrane, have largely been utilized over the past decade to study DNA with the intent of obtaining a fast and low-cost method for genome sequencing.[9−12] Although this is the ultimate target, this field continues to grow with significant achievements being made along the way in order to elucidate the reaction pathways of individual molecules,[13,14] their size and shape,[15] charge,[16−18] as well as other biophysical properties.[19] Perhaps more recently, researchers have started using a similar platform for the detection and investigation of other analyte

Received: January 20, 2011
Accepted: May 20, 2011
Published: May 20, 2011

molecules such as proteins.[14,19,20] Proteins are incredibly diverse and complex in terms of size, shape, and function. As a result, nanopores offer a unique and advantageous tool in the context of single-molecule analysis of proteins as the pore itself can be used as a physical barrier to unfold or stretch proteins. Importantly, a pore can also be used to manipulate the protein molecule based on changes in solvation,[21] mechanical force,[22] electric field,[23] and various solution conditions (chemical denaturants,[20] reduced pH,[24] elevated temperatures[25]). As a consequence, nanopores are well-suited for studying proteins under a large range of conditions at the single-molecule level.

For example, nanopores have recently been used to study the properties of bovine serum albumin (BSA) and were successful in estimating the size and charge of the folded state.[19] Others have performed a detailed study investigating the nonspecific adsorption of BSA to the pore surface.[14] Solid-state nanopores have also examined protein folding using β-lactoglobulin and urea as a denaturant.[20] However, the proposed mechanism of detection and the analysis that followed were based on the existence of stall points (i.e., where the protein would momentarily stop moving inside the pore). The protein−pore interaction is an interesting and important phenomenon whereby the protein sticks to the pore for a prolonged amount of time thereby increasing the resistance of the pore. On the basis of how the protein interacts with the pore (free translocation, single or multiple binding/sticking events), different physical interpretations of event duration can be employed. For example, the use of event duration has been used to calculate charge,[19] desorption rate constants,[26] and the effect of electroosmotic flow;[16] however, in all cases certain assumptions about how the protein interacts with the pore had to be made.

In this study, we show that BSA protein molecules either went through the pore with little interaction or interacted with the pore walls depending on the experimental denaturing conditions (thermal, chemical, and electric field) at low concentrations. This led to both short- and long-lived adsorption (and detection) events. Importantly, our studies simply take into account the current drop resulting in no assumptions being made with respect to the translocation time. We utilize these results in order to calculate the excluded volume of the protein under various denaturing conditions. Our results are also compared to those obtained by dynamic light scattering (DLS).

EXPERIMENTAL SECTION

Nanopore Fabrication. Nanopores were drilled in a 50 nm thick silicon nitride membrane which was supported on all sides by a square silicon support structure. Fabrication of this membrane consisted of first depositing a layer of low-stress silicon nitride on a silicon wafer using low-pressure chemical vapor deposition (LPCVD) followed by photolithography, deep reactive ion etching (DRIE), and KOH etching. The free-standing membrane, lying in the center of the silicon chip, was then put inside a transmission electron microscope (TEM; JEOL 2010F) for nanopore drilling. The tightly focused electron beam formed a 5 nm nanopore in less than 5 min, and by modifying the intensity of the electron beam using well-established techniques, pores could then be shrunk or expanded to the desired size.[27] Two different pore sizes were used during the course of this study: 10 and 30 nm.

The pore diameters were electrically characterized by measuring the current response given step increases in voltage. The

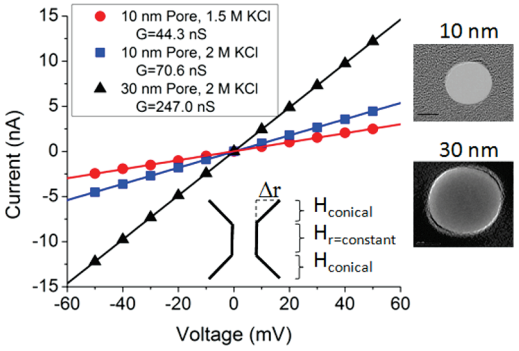

Figure 1. Electrical characterization of nanopores. The slope corresponds to the experimentally determined pore conductance, G (in nS). Insets show TEM images of a 10 and 30 nm pore (scale bars are 5 and 10 nm, respectively) and the internal profile of a pore with labeled model parameters.

resistance of the pore is given by the reciprocal of the slope obtained by plotting the mean current versus voltage. Resistance has the analytical form of $\Omega = \rho H/A = \rho H/\pi r^2$ where ρ is resistivity, A is the cross-sectional area of the pore, and H is the pore length. Since TEM-drilled pores have a well-characterized truncated double-cone structure,[27] the radius is a function of the z-height. Therefore, the resistance is evaluated by integrating $d\Omega = (\rho dz)/(\pi r^2)$ in three parts corresponding to r being a linear function of z, a constant value, and once again a linear function of z. Assuming the conical sections are symmetric, the total resistance can be simplified to

$$\Omega = 2(\Omega_{\text{conical}}) + \Omega_{r=\text{constant}} + \Omega_{\text{access}} = 2\left(\frac{\rho H_{\text{conical}}}{\pi r(r+\Delta r)}\right) + \frac{\rho H_{r=\text{constant}}}{\pi r^2} + \frac{\rho}{2r} \quad (1)$$

For the 10 nm pore and 1.5 M KCl, the analytical conductivity given by $G = 1/\Omega$ was calculated to be 40.0 nS, which when compared to the experimental value of 44.3 nS only amounts to a diameter change of 0.6 nm. For the 10 nm pore and 2 M KCl, the analytical conductivity was calculated as 50.0 nS, which is significantly lower than the experimental value of 70.6 nS. In order to fit the model to the experimental data, a pore size of 12 nm was used, which means the pore is conducting ions as if it were 2 nm larger. For the 30 nm pore, which has a lower aspect ratio, the contribution of access resistance becomes much more significant. Once again taking access resistance into account, the analytical conductance of 200 nS did not match the experimental value of 247 nS. However, in order to obtain an analytical conductance of 247 nS, a rather small diameter increase of 3 nm was sufficient to correct the discrepancy. The characterization of pore conductance using our mathematical model has shown that our nanopore sensors are conducting ions close to the values expected given the pore sizes obtained from TEM imaging (see Figure 1). Such small changes to the diameter can be attributed to assuming an internal profile that is perfectly symmetric and hourglass-shaped.

Nanopore Experiments. The methodology used for all nanopore experiments involved placing a single nanopore between two electrolytic half-cells which were filled with a potassium chloride solution (buffered at various pH values).[28] Protein molecules were then added to one half-cell and driven through the pore using an applied voltage (electric field strength varied

for each experiment) while ionic current was recorded using Ag/AgCl electrodes and an Axopatch recording system (Molecular Instruments). Protein translocation events were observed as transient decreases in the ionic current caused by the protein temporarily blocking the pore. The ionic current was filtered at 10 kHz and digitized (Digidata 1440, Molecular Instruments) at a sampling rate of 200 kHz. Data was collected over multiple experiments using the same nanopore, which was prepared prior to each experiment by treating with piranha solution (10 min) and plasma (5 min).

All protein solutions were diluted from a stock solution prior to each experiment in potassium chloride (1.5 or 2 M) to make a final protein concentration of 10 nM. For thermal unfolding experiments, the protein was diluted in a high-pH environment (pH 11.2, KCl/NaOH buffer) to maximize the net negative charge (the isoelectric point for BSA is 5.5). For a more complete description of how pH and KCl concentration affect protein charge and their effect on nanopore experiments, see the work of Firnkes et al.[16] Thermal denaturation was performed by placing the protein solution in a water bath set at 70 °C for 10 min and then cooling it to room temperature. For experiments that studied chemical denaturation and the effects of electric field strength, the solutions were buffered at pH 7 using potassium phosphate buffer. Chemical denaturation was accomplished using urea which was added to the protein solution to a final concentration of 8 M.

Dynamic Light Scattering Measurements. When a protein is inside a nanopore, the current drop parameter reflects both the volume of the protein as well as the hydration shell around the protein. Dynamic light scattering is a technique that takes into account such solvation effects and can be used to support nanopore results. DLS is a technique for sizing particles using Brownian motion in conjunction with the Stokes−Einstein relationship assuming spherical particles. Although BSA is ellipsoid-shaped in its native conformation, DLS can provide a relative measurement of protein size, which can be used to discriminate between different conformational states.[29] Protein solutions were prepared using the same protocol as used for nanopore experiments, however, at much higher concentrations (1 mM). However, due to expected aggregation at this concentration, thermally denatured BSA measurements were not compared to the nanopore data.[30] Measurements were performed on a Zetasizer Nano (Malvern Instruments).

Nanopore Data Analysis. The recorded electrical signals were analyzed using custom Matlab scripts which detected a translocation event based mainly on the current falling below a set threshold. Subsequent filtering steps removed artifacts and events which had unsteady baseline. Three event properties were extracted from the remaining events: duration (Δt), current drop (ΔI), and event area; however, the main event property we use here is the current drop. Both one- and two-dimensional data was fitted using Gaussian mixture models[31] where individual distributions were optimized using the maximum likelihood parameter and the number of distributions was determined by the minimization of the Akaike information.

RESULTS AND DISCUSSION

Thermal Effects on BSA. After thermally denaturing BSA, the solution was allowed to reach room temperature and was immediately injected into one chamber of the flow cell. Due to the negative charge of BSA at pH 11.2, once a positive voltage bias was applied to the electrode in the opposite chamber, transient decreases in current were recorded indicating that BSA was passing through the pore. Prior to adding protein, the ionic current was very stable and showed no transient decreases or drifts in the baseline value (7.3 ± 0.07 nA at 150 mV). Furthermore, no translocation events were observed when negative voltages were applied. The majority of translocation events were observed to have event properties similar to the representative event shown in Figure 2. These events had a mean translocation time of 0.077 ± 0.02 ms (n = 203) and 0.20 ± 0.05 ms (n = 120) along with a current drop of 0.99 ± 0.20 and 1.41 ± 0.25 nA, respectively. Events with durations longer than 350 μs (three standard deviations away from the nearest population) were classified as a long-lived event and occurred at a frequency of 12 events/min. For larger pores the frequency of these events decreased; however, larger voltages increased the frequency of the long-lived events, which has been described in detail previously.[14]

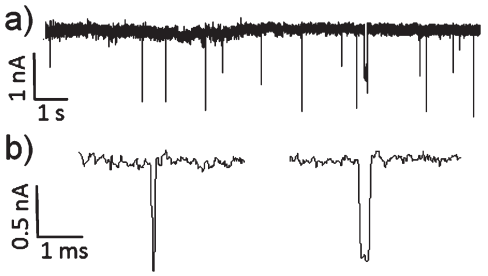

Figure 2. (a) Ionic current recording showing translocation events of thermally denatured and subsequently refolded BSA: voltage, 150 mV; pH, 11.2; KCl concentration, 1.5 M. (b) Two representative current blockades which were repetitively observed throughout the experiment. Experiments were conducted at 150 mV (baseline current = 7.3 nA).

A scatter plot of the translocation time versus event current drop (Figure 3) is used to view the distribution of points which make up two clusters corresponding to the two states of BSA. A Gaussian mixture model was then used to fit the two-dimensional data. A three-component model yielded the best fit of the data determined by the maximum likelihood parameter; however, the third component is composed mainly of outliers or background points which, based on the long event durations and the variability therein, represent translocation events where the protein interacted significantly with the pore. These long-lived events made up a small percentage of the total points and did not form tight cluster points in the scatter plot but rather produced a broad distribution of points. It is evident from the raw data as well as the Gaussian mixture model that the two main events types differ in both translocation duration and current drop.

Thermal denaturation of BSA is both a time- and temperature-dependent process which can result in reversible[25] or irreversible unfolding.[8,25,30] If irreversible unfolding occurs (starting at 50 °C) followed by bringing the solution back down to room temperature, BSA partially refolds but does not obtain its native conformation. Previous reports on temperature-based BSA unfolding have shown that the helicity of BSA (normally 66% or 385 out of its 583 residues) is reduced to approximately 42% when heated to 70 °C and then partially refolds to 58% helicity when cooled back to 25 °C.[25] Since the protein solutions prepared in this study were cooled before measurements, the refolded state was present rather than the completely unfolded form. Also, since BSA was left at 70 °C for only 10 min, every protein did not

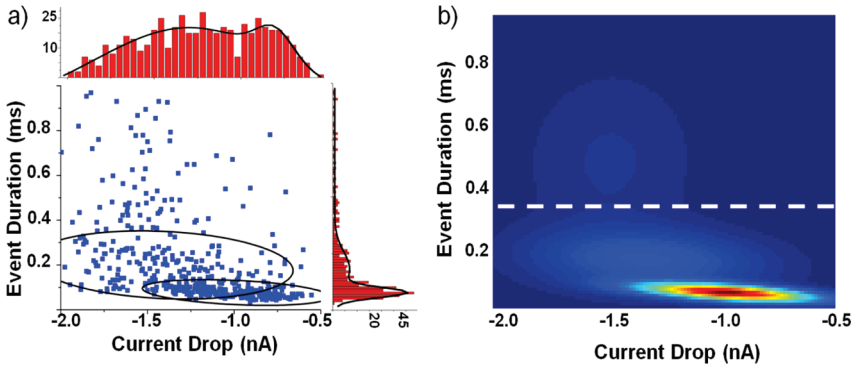

Figure 3. (a) Scatter plot displaying event duration (y-axis) and current drop (x-axis) properties for thermally denatured BSA (black curves, 3σ ellipses). The data was fitted using a Gaussian mixture model (b) which found two main populations and one characterized by long event durations suggesting protein−pore interaction or adsorption. Events longer than 350 μs (three standard deviations from the nearest population and marked by a dotted line) were classified into this long-lived event type. The two main populations had a mean translocation time of 0.077 ± 0.02 ms (n = 203) and 0.20 ± 0.05 ms (n = 120) along with a current drop of 0.99 ± 0.20 and 1.41 ± 0.25 nA, respectively.

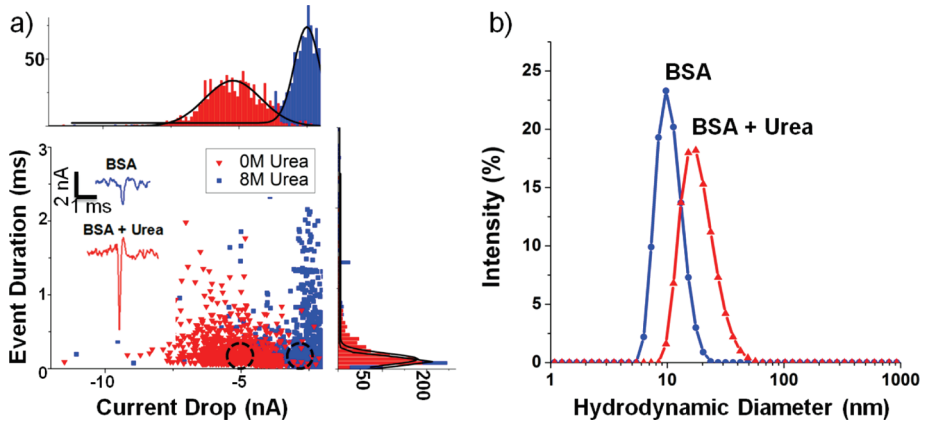

Figure 4. (a) Scatter plot, event duration, and current drop histograms and representative events for BSA without and with 8 M urea. The mean current drop values for BSA without urea and with urea were −3.0 ± 1.0 nA (n = 1973) and −5.3 ± 1.2 nA (n = 880), respectively. The duration parameter was not significantly different with values of 0.24 ± 0.24 and 0.25 ± 0.24 ms for BSA without and with urea, respectively. Inset: representative events with and without urea were chosen from within the circled regions (black dotted circles). Experiments were conducted at 300 mV (baseline current = 20.9 nA). (b) Hydrodynamic diameter measurements of BSA with and without urea using DLS: hydrodynamic diameter of BSA, 9.7 nm; BSA with urea, 22.7 nm (in 2 M KCl, 10 mM potassium phosphate buffer).

become thermally denatured, which means that some proteins remained in the native state.[30] In the present study, two types of events were detected which, based on the current understanding of BSA thermal unfolding, represent the thermally refolded and the thermally unaffected native states. At the pH 11.2 used here, the native state is also likely to be different than the native state at neutral pH since BSA slightly expands in response to the excess charge.[32] An alternative explanation for observing two event types is based on the formation of aggregates which was observed using DLS at high concentrations (1 mM). However, even if aggregates would form at such low concentrations over such short periods of time (10 min), only single BSA molecules should be able to fit through 10 nm nanopores.

Chemical Effects. Translocation events were recorded upon injecting BSA into one of the chambers of the flow cell while applying a voltage bias across the pore. The majority of experiments were performed at pH 7 which made each BSA molecule carry a net negative charge of −18 e. During initial experiments, natively folded BSA molecules were translocated through nanopores which measured 5, 10, and 20 nm in diameter. The 10 nm pore exhibited good signal-to-noise ratio, and the rate of long-lasting clogging events was manageable resulting in the most data being collected at this pore size. Therefore, the results in this section were obtained using a 10 nm pore and long-lasting events were filtered out prior to analysis.

The unfolding of BSA was investigated by using protein solutions which contained 0 and 8 M urea. By plotting these two data sets together, any shift in event properties would signify a structural change in the protein. The most significant change observed between folded and unfolded BSA was the current drop property (Figure 4a, P < 0.01). The mean current drop values for BSA without urea and with urea were −3.0 ± 1.0 nA (n = 1973) and −5.3 ± 1.2 nA (n = 880), respectively. The duration parameter was not significantly different with values of 0.24 ± 0.24 and 0.25 ± 0.24 ms for BSA without and with urea, respectively. An increase in the current drop means that a greater portion of the pore had become blocked when the protein was traveling through it. Unfolded proteins not only become less compact, their solvent-exposed surface area increases allowing more sites for hydration which can also increase the effective size of the protein.[29,33]

dx.doi.org/10.1021/ac2001725 |*Anal. Chem.* 2011, 83, 5137–5144

The similarity between folded and unfolded BSA event durations suggests that BSA does not freely translocate through the pore. If no protein−pore interactions occurred during translocation, the duration parameter would be related to the size and electrophoretic mobility of the protein, which is not the same for the folded and unfolded BSA molecule. The data suggests that, under these experimental conditions, BSA transiently binds to the pore surface during translocation, which explains why the duration parameter does not agree with free translocation theory. In experiments where protein−pore binding is studied, the event duration is directly related to the rate constant of desorption and has previously been studied.[26] In our analysis, different folding states of BSA were detected solely by means of the current drop parameter, which not only was sufficient in discriminating between folded and unfolded states but also allowed for excluded volume calculations.

In order to confirm that urea caused a shift in the effective size of BSA, a more traditional bulk protein measurement based on DLS was performed. The average size of folded and unfolded BSA was found to be 9.7 ± 1.8 and 22.7 ± 5.8 nm, respectively (Figure 4b). A value of 9.7 nm for folded BSA is reasonable since BSA is an ellipsoid molecule with dimensions of 4 × 4 × 14 nm^3.[19] However, the hydrodynamic diameter of urea-unfolded BSA should be viewed with more skepticism since the protein adopts an extended conformation, which can lead to overestimation of the overall size (if literally taken to mean "diameter"). The mass of a molecule is proportional to the hydrodynamic radius raised to a power equal to the mass fractal dimension, d_f ($m \propto r^{d_f}$).[34] For a rod, the mass fractal dimension is approximately 1 ($m \propto r^1$);[35] however, if incorrectly assumed to be spherical, the mass (or volume) would be calculated using r^3. Therefore, because the unfolded state does not have a well-defined structure, DLS is used here to confirm that the average conformation of urea-denatured BSA is distinct from that of the folded protein. It is also tempting to infer the existence of different protein conformations from the width of the DLS distribution; however, measurement variability and averaging over many measurements also affects the width. In addition, the measurement itself is an average of many molecules, and therefore, obtaining information about different protein conformations is hindered by ensemble averaging.

Electric Field Effects. One of the most critical parameters when studying proteins using nanopores is the applied voltage. The voltage not only determines how fast translocations occur (i.e., event duration) and the frequency of events but can also alter protein structure.[20,36] This is not true for DNA experiments because of its homogeneous negative charge. However, a protein exhibits a heterogeneous charge distribution along its backbone, which allows for individual amino acids to be pulled in opposite directions when an electric field is applied. This force on the amino acid side chains may cause structural instability and even denature the protein.[20] Furthermore, structural transformations have even been reported in electrophoresis experiments which are performed at much smaller electric field strengths.[20,36] Proteins have been studied before using nanopores; however, researchers have only commented on the fact that the structure may have been compromised by the electric field during their experiments. There has been no experimental data regarding how the change in protein structure might manifest itself in the recorded ionic current signal. Since experiments cannot be done in the absence of an electric field, the only option is to observe changes in the data by increasing the magnitude of the electric field.

Since few events were recorded below 300 mV, this was the lowest voltage at which data was collected. The applied voltage

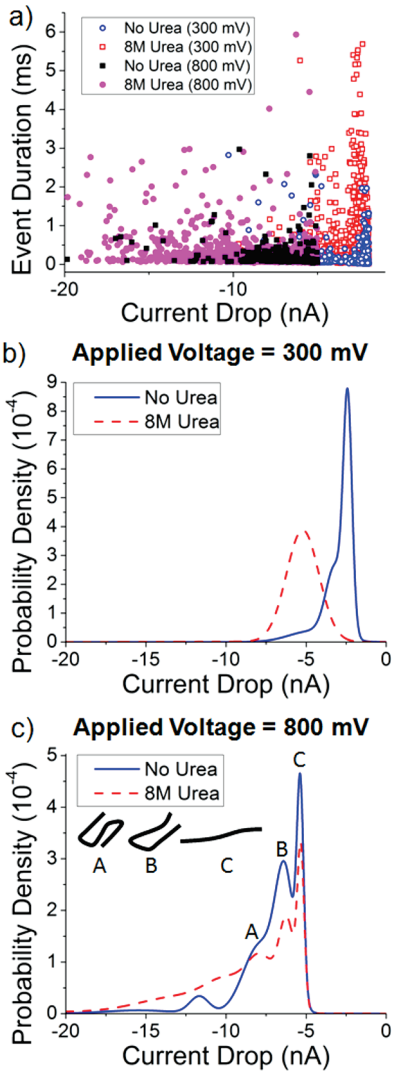

Figure 5. (a) Scatter plot of BSA translocation data with and without urea using applied voltages of 300 mV (n = 880 and n = 1973, respectively) and 800 mV (n = 1171 and n = 300, respectively). (b and c) Probability density functions for the current drop parameter obtained for BSA with and without 8 M urea using an applied voltage of (b) 300 and (c) 800 mV. KCl concentration, 2 M; pH, 7 (10 mM potassium phosphate buffer); nanopore diameter, 10 nm.

was then incrementally increased up to 900 mV where the pore started to become blocked. The largest quantity of data was collected at 800 mV; therefore, this potential was used to compare the results obtained at 300 mV (Figure 5). As the total number of detected events was different at both applied potentials, a probability density distribution was used to compare the results. The distributions at 300 mV showed only one main peak representing very reproducible and stable translocation events (Figure 5b). This is reasonable since BSA has an ellipsoid shape with the long axis being larger than the pore diameter suggesting that BSA translocations mainly occur in one orientation. The distributions for data recorded at 800 mV, however, showed multiple peaks (Figure 5c). We propose that these different peaks represent different conformational states populated by the protein. Interestingly, the same current drop was observed in both BSA samples (with and without urea) indicating that the effect of the electric field overrides that of urea. Taking these

dx.doi.org/10.1021/ac2001725 |Anal. Chem. 2011, 83, 5137–5144

Table 1. (a) On the Basis of the Excluded Volume Equation and BSA Translocation Data, the Effective Pore Length (nm) Was Calculated (Rightmost Column) Using the Known Excluded Volume of Folded BSA (117 nm^3); (b) Using the Experimentally Determined Pore Lengths, the Excluded Volumes of Refolded BSA, Urea-Denatured BSA, and Various Forms of BSA in an Electric Field Were Calculated (Rightmost Column)[a]

(a) Experimentally Determined Pore Lengths			
voltage (mV)	current drop (pA)	pore diameter (nm)	calculated pore length (nm)
150	990	10	17.3
300	2430	10	17
800	6120	10	17.5
300	2362	31	17.3
(b) Calculated Excluded Volumes of Unfolded BSA			
voltage (mV)	current drop (pA)	predicted protein state	excluded volume (nm^3)
150	1410	refolded	166 ± 29
300	5200	urea-denatured	250 ± 58
800	7870 (peak 1)	denatured by electric field	151 ± 3
800	6220 (peak 2)	denatured by electric field	119 ± 7
800	5435 (peak 3)	denatured by electric field	104 ± 6

[a] Excluded volumes are pH and KCl concentration dependent and are therefore specific to our experimental conditions (pH 11.2, KCl/NaOH buffer, 1.5 M KCl for the refolded protein state and pH 7, potassium phosphate buffer, 2 M KCl for the urea and electric field denatured protein states).

observations into account, a number of different translocation orientations can be envisioned which would produce these reproducible peaks (Figure 5c insets). Taking the length of an amino acid as 0.36 nm,[37] the length of fully extended BSA is approximately 210 nm. The conformation proposed for peak A would therefore have a length of 60−70 nm (one-third of the total length). If conformation A was "folded" any further, the entire protein would be within the sensing zone of the pore (a cylinder with a height and radius of 50 and 10 nm, respectively), which suggests that events to the left of peak A (including the small peak observed in the "No Urea" curve) represent events where the entire molecule is inside the nanopore. A well-defined peak with such a large current drop was only observed in the sample without urea, which could be due to the unique way in which the folded BSA molecule enters the pore prior to electric field-induced unfolding. The mean event durations for peaks A, B, and C were 206.8 ± 345, 187.3 ± 438, and 166.0 ± 354 μs, respectively, which suggests the most extended protein conformation travels through the pore quicker due to fewer interactions with the pore.

These results suggest that nanopores can be used as a new experimental tool to elucidate how the chemical and fluidic environments of proteins affect their propensity to be destabilized by electric fields. Electric field-induced unfolding is an interesting topic to study since proteins unfold by this mechanism inside cells;[38] however, for many experiments it may be desirable to prevent unfolding. For example, using native ligands or chemicals to stabilize protein structure (similar to how low concentrations of SDS stabilize BSA during thermal denaturation[39]) may prove critical to future experiments where structure needs to be maintained for either sensing protein biomarkers or protein binding in which the functional form would need to be maintained.

Excluded Volumes. The following equation, which is based on the original work by Deblois and Bean,[40] is used to estimate the excluded volume of a particle traveling through a pore:[20]

$$\text{excluded volume} \cong \frac{\Delta I_b (H_{eff})^2}{\sigma V} \qquad (2)$$

where ΔI_b is the current drop value, H_{eff} is the pore length, σ is the electrolyte conductivity, and V is the voltage. If this equation is applied to the folded form of BSA, whose structure and size are well-documented, the parameter which is least confidently known is H_{eff}. The membrane thickness, and thus the approximate length of the pore, is 50 nm. However, other factors come into play such as the geometry of the pore and access resistance (resistance outside of the pore), which reduces our ability to accurately prescribe a number to H_{eff}. Therefore, translocation data for folded BSA was used to experimentally determine H_{eff} and this value was then used to calculate the unknown excluded volume of unfolded BSA. Table 1 shows the experimental parameters used in eq 1 and the resulting H_{eff} values. Instead of averaging the H_{eff} values together, the H_{eff} value was selected based on pore size since the validity of underlying assumptions depend on the size of the pore.

For thermally denatured BSA, we concluded from our experiments that the population with the larger current drop corresponded to the refolded state of BSA. By first using data for folded BSA and its known excluded volume (117 nm^3, calculated using the volume of an ellipsoid), a pore length of 17.3 nm was found (Table 1). By using this value again in eq 1, the unknown excluded volume of the refolded BSA molecule was calculated to be 166 nm^3. Although the pore length was seemingly low compared to the actual membrane thickness (50 nm), the pore geometry of TEM-drilled pores has been described as an "hourglass" shape, which would reduce the effective pore length.[27] Furthermore, in the present work we are only interested in the relative increase in the excluded volume, which allows the pore length to be defined based on experimental data. If such data were not available, a more thorough analysis would have to be performed to accurately define this value. The pore length, calculated over larger pore sizes and voltages, yielded fairly consistent values between 17 and 17.5 nm (Table 1). Using H_{eff} for a 10 nm pore at 300 mV (17 nm), the excluded volume of urea-denatured BSA was calculated to be 250 nm^3, which is slightly more than double the size of its native conformation. From a model-based analysis of protein unfolding, we can expect

that the exposed surface area of the protein also is approximately twice that of the native state.[33] Due to the increase in exposed surface area and charged residues, it is expected that the observed volume increase is partially due to solvation effects (i.e., increased volume of the hydration shell). If the hydrodynamic radius obtained from DLS was used to estimate the excluded volume, assuming a sphere, the result would be a volume of 6125 nm^3, which is likely a drastic overestimation of the actual volume and is evidence for a nonspherical unfolded state.

At the larger applied voltage, the calculation of excluded volume is slightly more complicated since multiple peaks were observed. For the three main peaks in the current drop parameter (7.9 pA, 6.2 nA, 5.4 nA), the corresponding excluded volumes (in nm^3) were 151, 119, and 104. Interestingly, similar peaks were seen without urea, which suggests some common feature in the structure. One potential explanation is that the electric field was strong enough to nearly completely unfold the protein into an extended conformation, making the effects of urea very small inside the pore. If the protein conformation was fully extended, it would also block a smaller cross section of the pore causing the smaller than expected excluded volumes (compared to the urea-denatured state).

A comparison of these excluded volumes to other published data is unfortunately not possible for a number of reasons. First, we are not aware of any technique which measures the excluded volume of unfolded proteins. Second, it is extremely difficult to replicate the experimental conditions which exist inside a nanopore, particularly the electric field. Lastly, bulk measurements such as DLS require much higher concentrations which, when thermally denatured, causes rapid aggregation of BSA and prevents accurate measurement of individual protein molecules. However, by measuring the amount of ionic current being blocked by a single protein molecule, we directly obtain single-molecule excluded volumes. Nanopores may be a useful alternative to DLS and have the additional benefit of requiring lower concentrations and can overcome aggregation-related problems which hinder accurate excluded volume measurement of certain proteins.

SUMMARY AND CONCLUSION

In this paper we have investigated BSA under varying denaturing conditions using nanopores in order to broaden the scope of protein studies in the nanopore field. Moreover, we have shown how nanopores can be used to gain a fundamental understanding of how experimental parameters such as fluidic environment and applied voltage affect the molecules we are trying to observe and study. Finally, we calculated the excluded volumes of various conformational states of BSA including the thermally denatured and subsequently refolded state, the urea-denatured state, and multiple denatured conformations of BSA in the presence of an electric field (with and without urea).

AUTHOR INFORMATION

Corresponding Author

*E-mail: mkim@coe.drexel.edu.

ACKNOWLEDGMENT

The authors thank the following for financial support: HFSP young investigator award (RGY0075/2009-C).

REFERENCES

(1) Harsman, A.; Kruger, V.; Bartsch, P.; Honigmann, A.; Schmidt, O.; Rao, S.; Meisinger, C.; Wagner, R. *J. Phys.: Condens. Matter* **2010**, *22*, 454102.
(2) Movileanu, L.; Schmittschmitt, J. P.; Martin Scholtz, J.; Bayley, H. *Biophys. J.* **2005**, *89*, 1030–1045.
(3) Chansin, G. A. T.; Mulero, R.; Hong, J.; Kim, M. J.; deMello, A. J.; Edel, J. B. *Nano Lett.* **2007**, *7*, 2901–2906.
(4) Delehanty, J. B.; Ligler, F. S. *Anal. Chem.* **2002**, *74*, 5681–5687.
(5) Selkoe, D. J. *Nature* **2003**, *426*, 900–904.
(6) Walsh, D. M.; Hartley, D. M.; Kusumoto, Y.; Fezoui, Y.; Condron, M. M.; Lomakin, A.; Benedek, G. B.; Selkoe, D. J.; Teplow, D. B. *J. Biol. Chem.* **1999**, *274*, 25945–25952.
(7) Lansbury, P. T. *Proc. Natl. Acad. Sci. U.S.A.* **1999**, *96*, 3342–3344.
(8) Tobitani, A.; Ross-Murphy, S. B. *Macromolecules* **1997**, *30*, 4845–4854.
(9) Fologea, D.; Gershow, M.; Ledden, B.; McNabb, D. S.; Golovchenko, J. A.; Li, J. *Nano Lett.* **2005**, *5*, 1905–1909.
(10) Kasianowicz, J.; Brandin, E.; Branton, D.; Deamer, D. *Proc. Natl. Acad. Sci. U.S.A.* **1996**, *93*, 13770–13773.
(11) Storm, A. J.; Storm, C.; Chen, J.; Zandbergen, H.; Joanny, J.-F.; Dekker, C. *Nano Lett.* **2005**, *5*, 1193–1197.
(12) Ivanov, A. P.; Instuli, E.; McGilvery, C. M.; Baldwin, G.; McComb, D. W.; Albrecht, T.; Edel, J. B. *Nano Lett.* **2010**, *11*, 279–285.
(13) Howorka, S.; Movileanu, L.; Braha, O.; Bayley, H. *Proc. Natl. Acad. Sci. U.S.A.* **2001**, *98*, 12996–13001.
(14) Niedzwiecki, D. J.; Grazul, J.; Movileanu, L. *J. Am. Chem. Soc.* **2010**, *132*, 10816–10822.
(15) Li, J.; Gershow, M.; Stein, D.; Brandin, E.; Golovchenko, J. A. *Nat. Mater.* **2003**, *2*, 611–615.
(16) Firnkes, M.; Pedone, D.; Knezevic, J.; Döblinger, M.; Rant, U. *Nano Lett.* **2010**, *10*, 2162–2167.
(17) Keyser, U. F.; Koeleman, B. N.; van Dorp, S.; Krapf, D.; Smeets, R. M. M.; Lemay, S. G.; Dekker, N. H.; Dekker, C. *Nat. Phys.* **2006**, *2*, 473–477.
(18) Smeets, R. M. M.; Keyser, U. F.; Krapf, D.; Wu, M.-Y.; Dekker, N. H.; Dekker, C. *Nano Lett.* **2005**, *6*, 89–95.
(19) Fologea, D.; Ledden, B.; McNabb, D. S.; Li, J. *Appl. Phys. Lett.* **2007**, *91*, 053901–3.
(20) Talaga, D. S.; Li, J. *J. Am. Chem. Soc.* **2009**, *131*, 9287–9297.
(21) Lucent, D.; Vishal, V.; Pande, V. S. *Proc. Natl. Acad. Sci. U.S.A.* **2007**, *104*, 10430–10434.
(22) Carrion-Vazquez, M.; Oberhauser, A.; Fowler, S.; Marszalek, P.; Broedel, S.; Clarke, J.; Fernandez, J. *Proc. Natl. Acad. Sci. U.S.A.* **1999**, *96*, 3694–3699.
(23) Xu, D.; Phillips, J. C.; Schulten, K. *J. Phys. Chem.* **1996**, *100*, 12108–12121.
(24) Khan, M. *Biochem. J.* **1986**, *236*, 307–310.
(25) Moriyama, Y.; Watanabe, E.; Kobayashi, K.; Harano, H.; Inui, E.; Takeda, K. *J. Phys. Chem. B* **2008**, *112*, 16585–16589.
(26) Sexton, L. T.; Mukaibo, H.; Katira, P.; Hess, H.; Sherrill, S. A.; Horne, L. P.; Martin, C. R. *J. Am. Chem. Soc.* **2010**, *132*, 6755–6763.
(27) Kim, M. J.; McNally, B.; Murata, K.; Meller, A. *Nanotechnology* **2007**, *18*, 205302-6.
(28) Prabhu, A.; Jubery, T.; Freedman, K.; Mulero, R.; Dutta, P.; Kim, M. *J. Phys.: Condens. Matter* **2010**, *22*, 454107.
(29) Adel, A.; Nadia, M.; Mohamed, O.; Abdelhafidh, G. *Mater. Sci. Eng., C* **2008**, *28*, 594–600.
(30) Militello, V.; Vetri, V.; Leone, M. *Biophys. Chem.* **2003**, *105*, 133–141.
(31) Robertson, J. W. F.; Rodrigues, C. G.; Stanford, V. M.; Rubinson, K. A.; Krasilnikov, O. V.; Kasianowicz, J. J. *Proc. Natl. Acad. Sci. U.S.A.* **2007**, *104*, 8207–8211.
(32) Kun, R.; Szekeres, M.; Dékány, I. *J. Therm. Anal. Calorim.* **2009**, *96*, 1009–1017.
(33) Murphy, L. R.; Matubayasi, N.; Payne, V. A.; Levy, R. M. *Folding Des.* **1998**, *3*, 105–118.

(34) Bushell, G. C.; Yan, Y. D.; Woodfield, D.; Raper, J.; Amal, R. *Adv. Colloid Interface Sci.* **2002**, *95*, 1–50.
(35) Hyeon-Lee, J.; Beaucage, G.; Pratsinis, S. E.; Vemury, S. *Langmuir* **1998**, *14*, 5751–5756.
(36) Rochu, D.; Pernet, T.; Renault, F.; Bon, C.; Masson, P. *J. Chromatogr., A* **2001**, *910*, 347–357.
(37) Oesterhelt, F.; Oesterhelt, D.; Pfeiffer, M.; Engel, A.; Gaub, H. E.; Müller, D. J. *Science* **2000**, *288*, 143–146.
(38) Shariff, K.; Ghosal, S.; Matouschek, A. *Biophys. J.* **2004**, *86*, 3647–3652.
(39) Moriyama, Y.; Kawasaka, Y.; Takeda, K. *J. Colloid Interface Sci.* **2003**, *257*, 41–46.
(40) DeBlois, R. W.; Bean, C. P. *Rev. Sci. Instrum.* **1970**, *41*, 909–916.